PAPER • OPEN ACCESS

Asymmetry and inequity in the inheritance of a bacterial adhesive

IOP Publishing New J. Phys. 18 (2016) 045019 doi:10.1088/1367-2630/18/4/045019

New Journal of Physics
The open access journal at the forefront of physics

Deutsche Physikalische Gesellschaft DPG
IOP Institute of Physics

Published in partnership with: Deutsche Physikalische Gesellschaft and the Institute of Physics

OPEN ACCESS

RECEIVED
28 December 2015

REVISED
24 February 2016

ACCEPTED FOR PUBLICATION
11 March 2016

PUBLISHED
20 April 2016

PAPER

Asymmetry and inequity in the inheritance of a bacterial adhesive

Benjamin J Cooley[1], Sheri Dellos-Nolan[2], Numa Dhamani[1], Ross Todd[1], William Waller[1], Daniel Wozniak[1] and Vernita D Gordon[1,3]

[1] Center for Nonlinear Dynamics and Department of Physics, The University of Texas at Austin, Austin, Texas, USA
[2] Department of Microbiology, The Ohio State University, Columbus, Ohio, USA
[3] Institute for Cellular and Molecular Biology, The University of Texas at Austin, Austin, Texas, USA

E-mail: gordon@chaos.utexas.edu

Keywords: *Pseudomonas aeruginosa*, polysaccharide, Psl, Pel, adhesion, microscopy, symmetry

Abstract

Pseudomonas aeruginosa is an opportunistic human pathogen that forms biofilm infections in a wide variety of contexts. Biofilms initiate when bacteria attach to a surface, which triggers changes in gene expression leading to the biofilm phenotype. We have previously shown, for the *P. aeruginosa* lab strain PAO1, that the self-produced polymer Psl is the most dominant adhesive for attachment to the surface but that another self-produced polymer, Pel, controls the geometry of attachment of these rod-shaped bacteria—strains that make Psl but not Pel are permanently attached to the surface but adhere at only one end (tilting up off the surface), whereas wild-type bacteria that make both Psl and Pel are permanently attached and lie down flat with very little or no tilting (Cooley *et al* 2013 *Soft Matter* **9** 3871–6). Here we show that the change in attachment geometry reflects a change in the distribution of Psl on the bacterial cell surface. Bacteria that make Psl and Pel have Psl evenly coating the surface, whereas bacteria that make only Psl have Psl concentrated at only one end. We show that Psl can act as an inheritable, epigenetic factor. Rod-shaped *P. aeruginosa* grows lengthwise and divides across the middle. We find that asymmetry in the distribution of Psl on a parent cell is reflected in asymmetry between siblings in their attachment to the surface. Thus, Pel not only promotes *P. aeruginosa* lying down flat on the surface, it also helps to homogenize the distribution of Psl within a bacterial population.

Introduction

In biofilms, communities of interacting microbes are attached to a surface and to each other by a matrix of embedding, self-produced extracellular polymers (EPS). Biofilms help microbial infections become chronic by increasing the resistance of constituent organisms to the immune system and to antibiotics [1, 2]. In the initiating stages of biofilm development, some EPS constituents act as adhesins that stick individual microbes to the surface and to each other. A single bacterial strain can produce more than one type of EPS. The reasons for this redundancy are not well understood, but possibilities include providing a genetic backup plan in case of mutations [3], distinct roles for distinct EPS types [4, 5], and synergistic interactions between EPS types [5].

Pseudomonas aeruginosa is an opportunistic human pathogen that forms biofilm infections in host tissues and medical devices and is widely studied as a model organism for biofilm formation [6–8]. *In vitro*, the wild-type (WT) of the well-characterized *P. aeruginosa* lab strain PA01 makes two EPS, Psl and Pel. We have previously shown that Pel changes the geometry of adhesion so that rod-shaped *P. aeruginosa* cells are more likely to lie down flat on a surface [5]. This increases the fraction of the cell surface that is in contact with the substrate—i.e., the geometric coupling of the cell and substrate is increased. For *P. aeruginosa* and many other species of bacteria, the biofilm-promoting signaling molecule cyclic diguanylate (cyclic-di-GMP) is upregulated upon adhesion to a solid surface [9, 10]. The Wsp regulatory circuit is one system ultimately responsible for cyclic-di-GMP production [11, 12], and the surface-associated WspA proteins are distributed over the entire surface of the bacterial cell [13]. As a result, it seems likely that cells that are lying down flat should sense surfaces

better than cells that are attached at one end. Moreover, mechanosensing of solid surfaces by *P. aeruginosa* has recently been shown to upregulate virulence and signaling by cyclic-AMP [14, 15]. Extant approaches to preventing biofilms focus on developing surfaces that resist bacterial attachment or are bactericidal [16–19]. A better understanding of what properties are conferred by the expression of particular adhesins and how multiple types of EPS synergize should yield insight into what characteristics of surface adhesion promote pathogenesis, and thereby guide the development of new approaches for preventing or disrupting biofilms.

Here, we demonstrate a synergy between two EPS materials, Pel and Psl, in which Pel alters the distribution of Psl on the surfaces of rod-shaped *P. aeruginosa* cells. We find that Psl is distributed more uniformly along the lengths of WT cells than along isogenic Δ*pel* cells that are incapable of making Pel. In Δ*pel* populations, the Psl has a greater tendency to be concentrated at only one end of the cell. This is consistent with our previous finding that Δ*pel* populations have a strong tendency to be attached at only one end, tilting up off the surface, whereas WT populations are almost always lying flat on the surface, attached along the length of the cell body, and that Psl is by far the most important factor for bacterial adhesion to surfaces in these studies [5]. *P. aeruginosa* proliferates by increasing in length and then dividing across its minor axis, so altering the distribution of Psl along the major axis changes the way that the Psl from the parent is partitioned between the two daughters. We find that the geometry with which cells adhere to a flat, coverslip surface is reflective of epigenetic inheritance of Psl on the bacterial surface. These measurements are consistent with our measurements of Psl asymmetry using antibody staining. Therefore, we expect a more-uniform lengthwise distribution of Psl to result in a more-equitable inheritance of Psl by sibling cells. Symmetry and symmetry-breaking are fundamental concepts of physics. The adhesion characteristics we study here are examples of symmetry-breaking concepts from physics applied to an important biological system.

Materials and methods

The culturing of bacteria for phase-contrast microscopy was done as described in our previous work [5] and repeated here. This protocol was modified for antibody staining experiments, described below.

Bacteria and media

We used WT *P. aeruginosa* strain PAO1 [20] and three single-gene deletion strains in the PAO1 background, PAO1 Δ*pel* [21], PAO1 Δ*pelA* [22], and PAO1 Δ*psl* [23]. Δ*pel* is a polar mutant of *pelA* (i.e., polar mutation is a case such that mutation of a gene located upstream in the operon impacts the expression of genes in the same operon that are located downstream of the mutated gene); no substantial difference in the tilting behavior of Δ*pel* and Δ*pelA* was found.

Bacteria were streaked from frozen stock onto LB-Miller agar plates (5 g yeast extract, 10 g tryptone, 10 g sodium chloride, and 15 g agar per liter of Millipore water) and incubated at room temperature.

Rich media such as LB liquid medium (5 g yeast extract, 10 g tryptone, and 10 g sodium chloride per liter of Millipore water) have autofluorescence that can interfere with the fluorescence microscopy measurements described below. To avoid this, we use a defined, minimal medium (FAB) consisting of, in 1 L of Millipore water, 2 g $(NH_4)_2SO_4$, 9 g $Na_2HPO_4 \times 7H_2O$, 3 g KH_2PO_4, 3 g NaCl, 2 mL of $MgCl_2$ solution at 46.5 g L^{-1}, 1 mL of $CaCl_2 \times 2H_2O$ solution at 14 g L^{-1}, 1 mL of trace metals solution containing $CaSO_4 \times 2H_2O$ at 200 mg L^{-1}, $FeSO_4 \times 7H_2O$ at 200 mg L^{-1}, $MnSO_4 \times H_2O$ at 20 mg L^{-1}, $ZnSO_4 \times 7H_2O$ at 20 mg L^{-1}, $NaMoO_4 \times H_2O$ at 10 mg L^{-1}, and 0.2 mL of a second trace metals solution containing $CuSO_4 \times 5H_2O$ at 100 mg L^{-1}, $CoSO_4 \times 7H_2O$ at 50 mg L^{-1}, and H_3BO_3 at 25 mg L^{-1}. This is based on the medium used in Heydorn *et al* 2000 [24] and Shrout *et al* 2006 [25]. All chemicals were purchased from Sigma-Aldrich (USA).

Single colonies were inoculated into 4 ml FAB minimal medium with 36 mM disodium succinate as the sole carbon source and incubated at 37 °C in 20 mm glass culture tubes on an orbital shaker (Labnet Orbit 1000) with a 19 mm circular orbit operating at 200–250 rpm. Disodium succinate is added by filter sterilization; media with succinate is stored at 4 °C for no more than two weeks prior to use.

Sample growth

We grew the cultures in culture tubes to an optical density at 600 nm (OD_{600}) of 0.3, as measured by a Thermo Spectronic Genesys 20 Spectrophotometer. From our growth curve measurements, this corresponds approximately to mid-exponential growth phase.

Phase contrast microscopy

For time-lapse microscopy of tilting and cell motility we volumetrically diluted the culture, by adding sterile medium, by a factor of either 50 000× or 500 000×. We prepared samples for microscopy by placing an adhesive spacer (SecureSeal SS1X13) onto an uncoated glass slide, followed by addition of a few drops of the diluted

culture and covering with a glass cover slip to seal the chamber. Prior to use, we cleaned the cover slips by 5 min of sonication in a solution of 150 g of potassium hydroxide (KOH) dissolved in 450 mL of ethanol, followed by further sonication and rinsing in deionized water.

The bacteria were imaged using an Olympus IX71 inverted microscope in phase contrast mode. The microscope stage is enclosed within an incubator chamber heated to 30 °C. For better spatial resolution, monochromatic green light was used for illumination. We use a 60× oil-immersion objective in combination with an internal 1.6× multiplier that increases the effective magnification. Images were captured with a QImaging EXi Blue CCD camera controlled by a computer running QCapture Pro 6. An exposure time of 0.2 s and a frame rate of one frame per 30 s sufficed to capture most motion of the bacteria on the surface and avoid blurring. Rapidly spinning bacteria were excluded from the analysis. Images were assembled into time-lapse movies using the Fiji distribution of ImageJ software [26].

Thirteen time-lapse movies of Δ*pel* are reported on here. Our experiments began with a single isolated bacterium or a just-divided pair in the field of view. With time, bacterial division and attachment of additional cells caused the number of bacteria in the field of view to increase. The total number of bacteria surveyed per experiment was ∼10–60 over 4–6 h; daughter cells are counted as separate bacteria from the parent.

Structured illumination microscopy (SIM) experiments

For Psl staining experiments, we used an antibody for Psl. The antibody was conjugated directly to AlexaFluor 647. The bacteria were grown to an OD_{600} of 0.3, and then volumetrically diluted by a factor of 10 000× in sterile media with 1 mg mL^{-1} bovine serum albumin and 36 mM disodium succinate. The antibody was diluted in sterile media with no carbon, and then further diluted into the culture to a final dilution of 1:10 000. 500 μL of culture was transferred to a well of an 8-well chamber coverglass (Nunc Lab-Tek 155409). The culture was incubated for 1–2 h at 30 °C before imaging.

To achieve sub-cellular spatial resolution, we acquired SIM fluorescence images with a Zeiss Elyra S.1 microscope. We used a 63× oil-immersion objective lens, and the bacteria were illuminated with a 642 nm laser. We acquired three-dimensional *z*-stack images with a depth of ∼2.5–3.5 μm and a spacing of 144 nm. The raw image stacks were processed using the Zeiss ZEN software to arrive at the final high-resolution, 3D images of the bacteria.

Immunoblotting

The immunoblotting procedure was done as in [27]. In brief, cultures were pelleted to concentrate cells, which were re-suspended in EDTA, boiled, centrifuged, treated with proteinase, and stored at 4 °C for subsequent immunoblotting. The resulting polysaccharide preparations were normalized to have equal protein concentrations (to ensure that the total culture contribution to each sample was equal) and then spotted onto a nitrocellulose membrane, blocked, and probed with *a*-Psl antibody conjugated directly to AlexaFluor 647, diluted to a concentration of 1:10 000.

Analysis—phase contrast

The phase contrast microscopy movies were analyzed by hand to find instances of tilting, measure lifetime of each bacterium (division to division), and track the lineage of each bacterium. We define the bacteria present at the start of the movies as generation 1, their daughter cells as generation 2, and so forth. Between three and six generations were analyzed for each movie.

Phase contrast movies were also tracked using a version of colloid-tracking software [28] modified to account for elongated particles rather than spherical ones [29]. Tracking output includes center position, velocity, orientation in the focal plane, and the aspect ratio, projected onto the focal plane, of each bacterium. To exclude poorly-tracked bacteria, we only consider bacteria tracked for more than five minutes.

As a proxy readout for tilting, we look at the projected aspect ratio in each frame. A newly-divided cell lying flat on the surface has an aspect ratio of about 2.5. Therefore, a projected aspect ratio less than 2.5 indicates unambiguously that a cell is tilting. Interpretation of aspect ratios larger than 2.5 is ambiguous, since these cells may be either lying flat or longer cells tilted up. For each cell, we then compute the fraction of its lifetime spent unambiguously tilting, with 1 being unambiguously tilted up for the whole trajectory and 0 lying flat for the whole trajectory.

Analysis—sim

We made Z-projections of individual bacteria from processed SIM stacks, including ∼3 slices of the top side of each bacterium. Asymmetry in the staining was found by bisecting the image of the bacterium along the minor axis, finding the mean intensity of each half, and taking the ratio of brighter half to dimmer half.

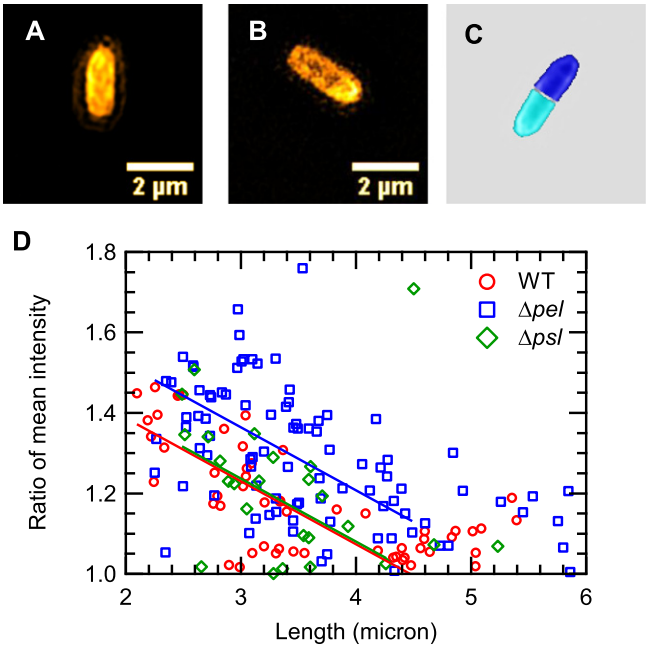

Figure 1. Pel increases the homogeneity of the distribution of Psl on the cell surface. (A) WT and (B) Δ*pel* bacteria fluorescently stained using an antibody for Psl and imaged using high-resolution SIM. (C) For analysis, we bisect the image of each bacterium along its minor axis and measure the asymmetry in Psl distribution by taking the ratio of the mean intensity of the two halves of the bacterium. Higher ratios correspond to greater asymmetry. (D) For each strain these ratios decrease with increasing bacterial length. For Δ*pel*, ratios are higher than for WT and Δ*psl*, as shown by the trendlines. The slope from the least-squares linear fit for WT data was used for fitting the data from Δ*pel* and Δ*psl*. Thus, the shift in *y*-intercept measures the difference in asymmetry between strains. Scale bars, 2 μm.

Results and discussion

Pel makes the distribution of Psl on cell surfaces more symmetric

P. aeruginosa is rod-shaped. We have previously shown that Δ*pel* is more likely to tilt up off the surface, attached by only one end, than is the WT, which tends to lie flat on the surface [5]. We have previously shown that Psl is more important than Pel, pili, or flagella for adhesive interactions between PAO1 single cells and a coverslip surface; without Pel, Psl-mediated adhesion will tend to have cells attached to the surface by only one end, but without Psl, Pel-mediated adhesion allows half the bacterial population to escape the surface [5]. Therefore, we infer that Pel is likely to promote lying down flat, i.e. tighter geometric coupling, by increasing the homogeneity of the Psl coating on the surface of the cell. To evaluate this inference, we label bacteria with a fluorescent antibody for Psl and image using high-resolution SIM (figures 1(A) and (B)). We measure the inhomogeneity of Psl distribution on bacterial cell surfaces by taking the ratio of the brightness of the two halves of each bacterium (figure 1(C)). We find greater asymmetry in the distribution of Psl on the Δ*pel* than on the WT (figure 1(D)). Taking the median of the measured length, ~3.4 μm, as a threshold and a proxy for the midpoint in the cell life-cycle, we can compare the asymmetry in 'young' (shorter than 3.4 μm) and 'old' (longer than 3.4 μm) bacteria. For young WT, the mean ratio is 1.25 $\pm$ 0.02, where the uncertainty is the standard error of the mean. For young Δ*pel* the ratio is 1.37 $\pm$ 0.02, 10% more asymmetric than the young WT. For old WT and Δ*pel* the ratios are 1.08 $\pm$ 0.01 and 1.22 $\pm$ 0.02, respectively—a 13% difference. Old Δ*pel* bacteria show roughly the same asymmetry as do young WT.

Ambiguity in the immunostaining

In our SIM experiments with immunostained bacteria we tested WT, Δ*pel*, and Δ*psl* (figure 1). We found that even Δ*psl* bacteria could be imaged, and that their brightnesses were comparable to those of WT and Δ*pel*. This indicates that the immunostain was not perfectly specific to Psl. To evaluate the degree of non-specificity, we performed immunoblotting using the fluorophore-conjugated Psl antibody. Polysaccharides from both WT and Δ*psl* made visible immunoblots, but the WT blot is much darker, indicating that it contains more material (figure 2). From this result we conclude that the antibody stain has a greater affinity for Psl than it does for its non-specific target(s). Furthermore, for Δ*psl*, we find the asymmetry in staining is unchanged from that of the WT (figure 1(D)). Therefore, in our analysis and discussion of our immunostaining results we compare WT and

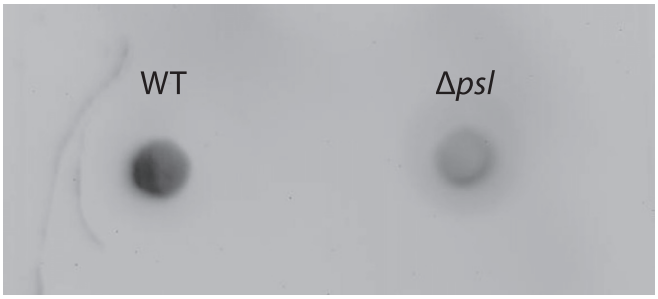

Figure 2. Immunoblots reveal nonspecificity for Psl. We performed immunoblotting using the fluorophore-conjugated Psl antibody. Polysaccharides from both WT and Δ*psl* show visible immunoblots, but the WT blot is much darker, indicating that it contains more material. From this result this we conclude that the antibody stain has a greater affinity for Psl than it does for its non-specific target(s).

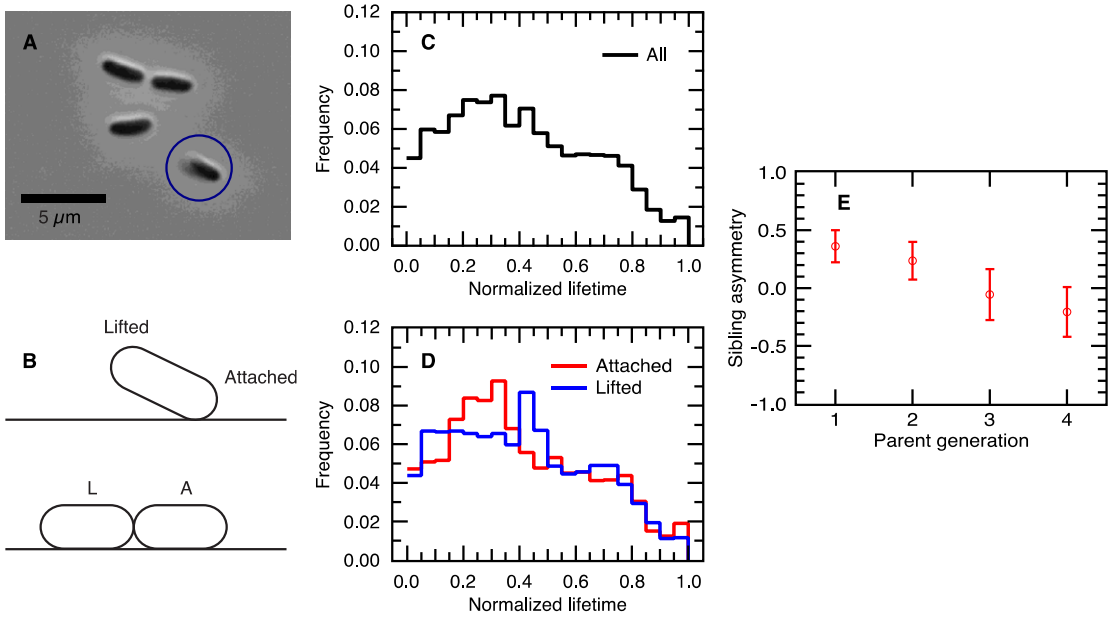

Figure 3. The likelihood of tilting depends on bacterial age and inheritance from the parent. (A) Phase contrast micrograph of four Δ*pel* cells; the lower right bacterium is tilting (the end above the surface is out of focus). (B) One end of a parent bacterium will spend more time lifted off the surface than the other end. We classify daughter cells by whether they originated from the lifted end 'L' or the attached end 'A' of the parent. (C) Bacteria are more likely to tilt in the early stages of life than in the later stages. (D) This is true regardless of whether the bacteria came from the attached or the lifted side of the parent, consistent with decreasing Psl asymmetry as bacteria age. (E) For the first two generations after the start of observation, L daughters spend more time tilting than do their A siblings.

Δ*pel*, which we expect to have similar non-specific staining, and we interpret differences between these strains as resulting from changes in Psl distribution.

We further check that interpretation by measuring how the likelihood of tilting by Δ*pel* depends on bacterial age and parental inheritance of Psl that we infer from our immunostaining. We have previously shown that Psl is the most important factor allowing PAO1 to adhere to the surface [5]. Furthermore, our SIM results (figure 1(D)) show that WT, which spend nearly all their time lying flat on the surface, have less asymmetry in their Psl distribution than do Δ*pel*, which are much more likely than WT to be attached at only one end [5]. Therefore, we expect that Δ*pel* bacteria will be more likely to attach at only one end when the asymmetry in Psl distribution is high—i.e., young (short) bacteria will be more likely to tilt than will older (long) bacteria (figure 1(D)). We identify tilting bacteria by one end being out of focus (figure 3(A)). Indeed, we find that the likelihood of tilting decreases with bacterial age (figures 3(C) and (D)).

Furthermore, Δ*pel* bacteria whose parent tilted spend, on average, 8.1 $\pm$ 0.8 min tilting, whereas those whose parent never tilted spend, on average, only 3.8 $\pm$ 1.9 min. This is a twofold difference in the likelihood of tilting and is consistent with the picture that daughters from a parent coated with more Psl, and therefore less likely to tilt, will have inherited more Psl than those from a parent coated with less Psl. We investigate tilting, as a proxy for Psl inheritance, using the genealogy of daughter cells. Most tilting bacteria have one end (the 'lifted' end) that spends more time off the surface than does the other end (the 'attached' end) (figure 3(B)). We expect

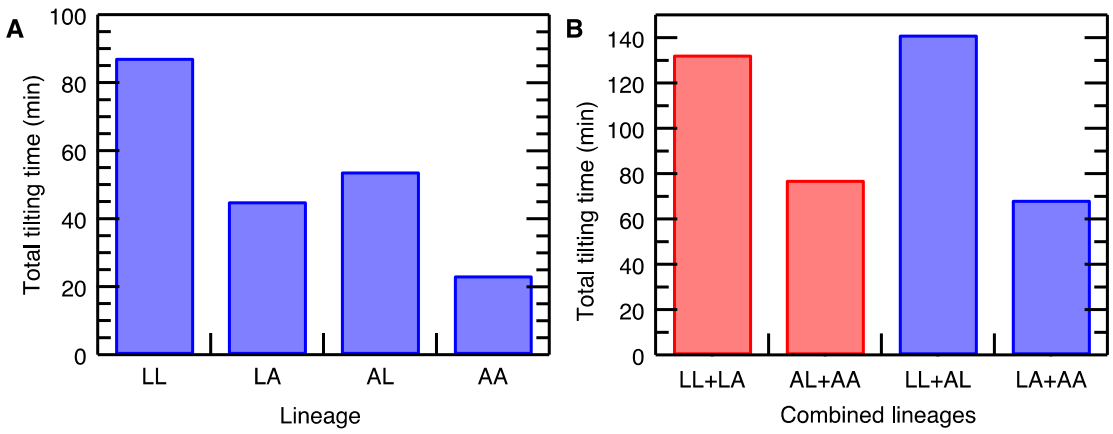

Figure 4. A tendency toward tilting can be inherited from the grandparent as well as the parent. (A) Total times spent tilting, sorted by whether the cell came from the lifting 'L' or attached 'A' ends of the grandparent and parent. Cells from two generations of lifted ends (LL) spend nearly 4× more time tilting than cells from two generations of attached ends (AA). Cells from the lifted end of the grandparent and the attached end of the parent (LA) and cells from the attached end of the grandparent and the lifted end of the parent (AL) spend intermediate amounts of time tilting. (B) Cells from the lifted side of the grandparent (LL and LA) spend 1.71× more time tilting than do cells from the attached side of the grandparent (AL and AA). Red bars compare the effect of lineage from the grandparent. The effect of lineage from the parent, shown in blue bars, is comparable: cells from the lifted side of the parent (LL and AL) spend 2.05× more time tilting than do cells from the attached side of the parent (LA and AA).

that the attached end of a bacterium should be coated with more Psl than the lifted end. As a result siblings will inherit different amounts of Psl. To measure the asymmetry in the time spent tilting by siblings, we pairwise compare the amount of time spent tilting by the daughter from the parent's lifted end 'L' with the amount of time spent tilting by the daughter from the attached 'A' end (figure 3(B)). We define a sibling asymmetry parameter

$$\alpha_{\mathrm{LA}} = (F_{\mathrm{L}} - F_{\mathrm{A}})/(F_{\mathrm{L}} + F_{\mathrm{A}}),$$

where $F_{\mathrm{L,A}}$ measures the number of frames spent tilting by the L, A siblings. A positive, nonzero value indicates that the L sibling spends more time tilting. We average over all such sibling pairs in each generation, where we have defined 'generation' such that the bacteria on the surface at the start of imaging are generation 1, their daughters generation 2, etc. For the first two generations the L daughters spend more time tilting than do the A daughters (figure 3(E)). From this we conclude that the A siblings inherit more Psl than their paired L siblings. This asymmetry disappears in later generations, perhaps due to conditioning of the surface as the bacteria shed Psl [30].

Because Psl promotes its own production by upregulating cyclic-di-GMP signaling [31], we expect tilting characteristics to be passed on to granddaughters as well as to daughters. For these comparisons we restrict ourselves to quartets of granddaughters for which both of the middle generation bacteria tilted. There were 13 such sets in the movies we examined. We sort the bacteria based on whether they descended from the lifted 'L' or attached 'A' end of their grandparent and parent. Our nomenclature describes the grandparent end 'G' first and the parent end 'P' second, thus: GP. For example, an AL bacterium came from the lifted end of its parent, which in turn came from the attached side of the grandparent. We sum the total tilting time for all four categories (LL, LA, AL, and AA) and find that the granddaughters from two generations of lifted ends (LL) tilt over three times as much as the granddaughters that from two generations of attached ends (AA) (figure 4(A)). The mixed granddaughters, LA and AL, fall in between. These data indicate that the tilting traits of grandparents, as well as parents, can be inherited. To compare the degree to which parental and grandparental inheritance impacts granddaughters, we group our data in two different ways: by which end of the grandparent they came from and by which end of the parent they came from. We find that bacteria from the lifted end of the grandparent tilt ~1.7 times as much as bacteria from the attached end of the grandparent (figure 4(B), red bars). In comparison, bacteria from the lifted end of the parent tilt ~2.1 times as much as bacteria from the attached end of the parent (figure 4(B), blue bars). These results indicate that parental and grandparental inheritances have comparable impact on the tilting behavior of bacteria. This is consistent with the connection we propose between tilting, Psl distribution, and cyclic-di-GMP signaling.

To assess whether there is any pattern in the subcellular localization of Psl on Δ*pel* cells, we turn to symmetry-breaking. To phase-contrast optical microscopy, *P. aeruginosa* is a symmetric rod. Below this length scale, the most prominent symmetry-breaking structural component is a single polar flagellum. Others have previously shown that flagella can act as adhesins for *P. aeruginosa* [32]. We hypothesize that there is more Psl on the flagellated ends of Δ*pel* than on the unflagellated ends, and we test this by determining which part of the

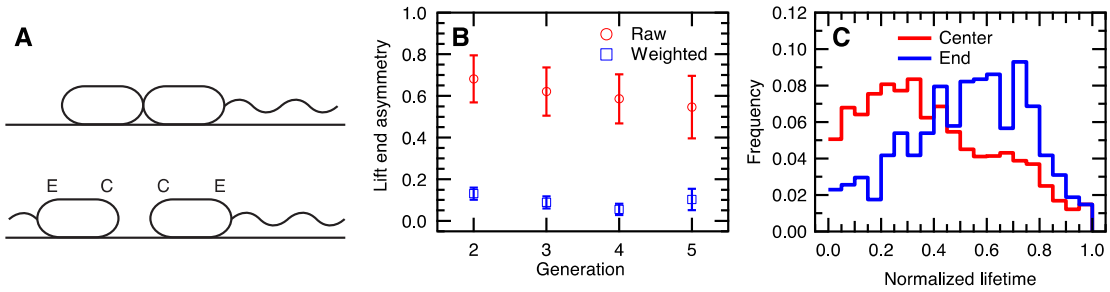

Figure 5. Bacteria are more likely to lift the end of the cell that originated from the center. (A) Cartoon of bacterium dividing, seen from the side. (B) Asymmetry in the lifted end of individual cells, which remains pronounced across generations. Positive values indicate the cells spend more time lifting the C end. (C) Bacteria lifting the C end (red line) tend to tilt earlier in life than do bacteria lifting the E end (blue line). Histograms are normalized.

parent cell is most likely to give rise to the lifted end. Previous researchers have found that after division one daughter cell retains the parent's flagellum, and the other daughter grows a new flagellum from the end that was not the center of the parent [33] (figure 5(A)). Therefore, we expect to find that the end that came from the center of the parent cell should be more likely to be the lifted end. We define a center-end asymmetry parameter

$$\alpha_{\mathrm{CE}} = (F_{\mathrm{C}} - F_{\mathrm{E}})/(F_{\mathrm{C}} + F_{\mathrm{E}}),$$

where $F_{\mathrm{C,E}}$ measures the number of frames in which the ends that came from the parent center 'C' and end 'E' lift, respectively. A positive, nonzero value indicates that the end that came from the parent center lifted more. Averaging within each generation, we find that C is 5× more likely than E to be the lifted end (figure 5(B), red circles). To account for individual differences in the amount of time that cells spend tilting, we weight each individual asymmetry by the fraction of the bacteria's lifetime that was spent tilting. This defines a weighted center-end asymmetry parameter

$$\alpha_{\mathrm{W}} = (F_{\mathrm{tilt}}/F_{\mathrm{all}})\alpha_{\mathrm{CE}},$$

where F_{tilt} is the number of frames the bacterium spends tilting and F_{all} is the total number of frames in the bacterium's lifetime. The resulting values remain well-resolved from zero for all generations (figure 5(B), blue squares).

Revisiting time evolution of tilting over bacterial lifetime, cells that primarily lift the C end follow the same trend as the population overall, tilting more when young (figure 5(C), red line). However, bacteria that lift the E end tilt less in the first half of their life than in the second half (figure 5(C), blue line). We suggest that lifting the E end of a young bacterium may be unlikely due to the asymmetric distribution of Psl, and that it becomes easier for the E end to lift later in life as this asymmetry decreases (figure 1(D)). These data are consistent with, but not proof positive of, the hypothesis that the flagellated end of the bacterium is the end most likely to be adhered to the surface and the end that has more Psl. Alternatively, polar Type IV pili could act to break the symmetry between C and E ends of the bacteria [34].

Discussion

Symmetry and symmetry-breaking are fundamental themes more commonly seen in traditional fields of physics than in biological physics. Understanding the interaction(s) that lead to symmetry being broken will often yield new insight into a system. Here we present a case of observed broken symmetry in a biological system and show how that was used to understand the underlying, symmetry-breaking biology. Tilting behavior in PAO1 Δ*pel* is asymmetric between ends of the bacteria as well as between siblings from a tilting parent, and the tilting behavior of a given cell can influence at least two generations of descendants. Most tilting occurs by lifting the end that was the center of the parent, and tilting by lifting the edge end tends to happen later in the bacterium's division cycle, as we surmise the distribution of Psl becomes more symmetric along the length of the bacterium.

Irie *et al* have shown that extracellular Psl is a signal that stimulates cyclic-di-GMP production [31]. In this light, our results suggest that heritability of asymmetries in Psl distribution may allow Psl to act as an epigenetic factor influencing daughter cells' cyclic-di-GMP levels after cell division. Because elevated cyclic-di-GMP level is also a signal to produce Psl, a positive feedback loop is formed for individual cells. This suggests that Psl asymmetry in individual cells, as well as across a population, should propagate and increase as cells divide. However, for planktonic *P. aeruginosa* it has been shown that, immediately post-septum formation, the flagellated sibling has more than 5× lower cyclic-di-GMP levels than the non-flagellated sibling [33]. These observations indicate that other factors carry additional weight in determining intracellular cyclic-di-GMP level.

More broadly, it indicates that regulation of symmetry and asymmetry may be a broad theme underlying early biofilm development.

Pel was recently found to be a polycation composed of partially-acetylated amino sugars, N-acetylgalactosamine and N-acetylglucosamine [35], but the specifics of its molecular structure are not known. In our earlier work, we speculated that Pel likely had a synergistic interaction with Psl, perhaps *via* cross-linking and/or another chemical interaction [5]. Our finding here that loss of Pel production results in a redistribution of Psl on the cell surface is also consistent with that speculation. Unfortunately, without a molecular-level understanding of how Psl and Pel interact, this cannot be confirmed or refuted, nor can its dependence on carbon source or other environmental conditions be assessed other than by further empirical studies. This could be a fruitful direction for future studies to assess the impacts of polysaccharides on bacterial adhesion mechanics, and possibly on intracellular cyclic-di-GMP regulation as discussed in the previous paragraph.

Acknowledgments

We thank Professor Matthew Parsek (University of Washington, Seattle) for his generous gift of bacterial PAO1 strains. We also thank Professor Marvin Whiteley (University of Texas at Austin) for WT and Δ*psl* polysaccharide preparations. SIM imaging (for figure 1) was performed in the Microscopy Core Facility within the Institute for Cellular and Molecular Biology at UT Austin, with the assistance of Julie Hayes. This work was funded by startup funds from UT Austin and a gift from ExxonMobil to VDG, and by a grant from the Human Frontiers Science Program (HFSP RGY0081/2012-GORDON).

References

[1] Parsek M R and Singh P K 2003 Bacterial biofilms: an emerging link to disease pathogenesis *Annu. Rev. Microbiology* **57** 677–701
[2] Costerton J W, Stewart P S and Greenberg E P 1999 Bacterial biofilms: a common cause of persistent infections *Science* **284** 1318–22
[3] Colvin K *et al* 2012 The Pel and Psl polysaccharides provide *Pseudomonas aeruginosa* structural redundancy within the biofilm matrix *Environ. Microbiology* **14** 1913–28
[4] Colvin K M *et al* 2011 The Pel polysaccharide can serve a structural and protective role in the biofilm matrix of *Pseudomonas aeruginosa* *PLoS Pathog.* **7** e1001264
[5] Cooley B *et al* 2013 The extracellular polysaccharide Pel makes the attachment of *P. aeruginosa* to surfaces symmetric and short-ranged *Soft Matter* **9** 3871–6
[6] O'Toole G A 2003 To build a biofilm *J. Bacteriology* **185** 2687–9
[7] Ryder C, Byrd M and Wozniak D J 2007 Role of polysaccharides in *Pseudomonas aeruginosa* biofilm development *Curr. Opin. Microbiology* **10** 644–8
[8] Mann E E and Wozniak D J 2012 Pseudomonas biofilm matrix composition and niche biology *FEMS Microbiology Rev.* **36** 893–916
[9] Cotter P and Stibitz S 2007 c-di-GMP-mediated regulation of virulence and biofilm formation *Curr. Opin. Microbiology* **10** 17–23
[10] Hengge R 2009 Principles of c-di-GMP signalling in bacteria *Nat. Rev. Microbiol.* **7** 263–73
[11] Güvener Z T and Harwood C S 2007 Subcellular location characteristics of the *Pseudomonas aeruginosa* GGDEF protein, WspR, indicate that it produces cyclic-di-GMP in response to growth on surfaces *Mol. Microbiology* **66** 1459–73
[12] O'Connor J R, Kuwada N J, Huangyutitham V, Wiggins P A and Harwood C S 2012 Surface sensing and lateral subcellular localization of WspA, the receptor in a chemosensory-like system leading to c-di-GMP production *Mol. Microbiology* **86** 720–9
[13] Huangyutitham V, Güvener Z T and Harwood C S 2013 Subcellular clustering of the phosphorylated WspR response regulator protein stimulates its diguanylate cyclase activity *mBio* **4** e00242–13
[14] Siryaporn A, Kuchma S L, O'Toole G A and Gitai Z 2014 Surface attachment induces *Pseudomonas aeruginosa* virulence *Proc. Natl. Acad. Sci. USA* **111** 16860–5
[15] Persat A, Inclan Y F, Engel J N, Stone H A and Gitai Z 2015 Type IV pili mechanochemically regulate virulence factors in *Pseudomonas aeruginosa Proc. Natl. Acad. Sci. USA* **112** 7563–8
[16] Glinel K, Thebault P, Humblot V, Pradier C and Jouenne T 2012 Antibacterial surfaces developed from bio-inspired approaches *Acta Biomater.* **8** 1670–84
[17] Salwiczek M *et al* 2014 Emerging rules for effective antimicrobial coatings *Trends Biotechnol.* **32** 82–90
[18] Graham M and Cady N 2014 Nano and microscale topographies for the prevention of bacterial surface fouling *Coatings* **4** 37–59
[19] Tan S Y-E, Chew S, Tan S Y-Y, Givskov M and Yang L 2014 Emerging frontiers in detection and control of bacterial biofilms *Curr. Opin. Biotechnol.* **26** 1–6
[20] Holloway B W, Krishnapillai V and Morgan A F 1979 Chromosomal genetics of Pseudomonas *Microbiol. Rev.* **43** 73–102
[21] Borlee B R *et al* 2010 *Pseudomonas aeruginosa* uses a cyclic-di-GMP-regulated adhesin to reinforce the biofilm extracellular matrix *Mol. Microbiol.* **75** 827–42
[22] Starkey M *et al* 2009 *Pseudomonas aeruginosa* rugose small-colony variants have adaptations that likely promote persistence in the cystic fibrosis lung *J. Bacteriology* **191** 3492–503
[23] Kirisits M J, Prost L, Starkey M and Parsek M R 2005 Characterization of colony morphology variants isolated from *Pseudomonas aeruginosa* Biofilms *Appl. Environ. Microbiol.* **71** 4809–21
[24] Heydorn A *et al* 2000 Quantification of biofilm structures by the novel computer program comstat *Microbiology* **146** 2395–407
[25] Shrout J *et al* 2006 The impact of quorum sensing and swarming motility on *Pseudomonas aeruginosa* biofilm formation is nutritionally conditional *Mol. Microbiology* **62** 1264–77
[26] Schindelin J *et al* 2012 Fiji: an open-source platform for biological-image analysis *Nat. Methods* **9** 676–82
[27] Huse H K *et al* 2013 *Pseudomonas aeruginosa* enhances production of a non-alginate exopolysaccharide during long-term colonization of the cystic fibrosis lung *PLoS One* **8** e82621
[28] Crocker J C and Grier D G 1996 Methods of digital video microscopy for colloidal studies *J. Colloid Interface Sci.* **179** 298–310

[29] Conrad J C et al 2011 Flagella and pili-mediated near-surface single-cell motility mechanisms in P. aeruginosa Biophys. J. 100 1608–16
[30] Zhao K et al 2013 Psl trails guide exploration and microcolony formation in Pseudomonas aeruginosa biofilms Nature 497 388–91
[31] Irie Y et al 2012 Self-produced exopolysaccharide is a signal that stimulates biofilm formation in Pseudomonas aeruginosa Proc. Natl. Acad. Sci. USA 109 20632–6
[32] Haiko J and Westerlund-Wikström B 2013 The role of the bacterial flagellum in adhesion and virulence Biology 2 1242–67
[33] Christen M et al 2010 Asymmetrical distribution of the second messenger c-di-GMP upon bacterial cell division Science 328 1295–7
[34] Skerker J and Berg H 2001 Direct observation of extension and retraction of type IV pili Proc. Natl. Acad. Sci. USA 98 6901–4
[35] Jennings L et al 2015 Pel is a cationic exopolysaccharide that cross-links extracellular DNA in the Pseudomonas aeruginosa biofilm matrix Proc. Natl. Acad. Sci. USA 112 11353–8